



HAL
open science

Nanostructure and photocatalytic properties of TiO₂ films deposited at low temperature by pulsed PECVD

D. Li, S. Bulou, N. Gautier, S. Elisabeth, A. Goulet, M. Richard-Plouet, P. Choquet, A. Granier

► To cite this version:

D. Li, S. Bulou, N. Gautier, S. Elisabeth, A. Goulet, et al.. Nanostructure and photocatalytic properties of TiO₂ films deposited at low temperature by pulsed PECVD. Applied Surface Science, 2019, 466, pp.63-69. 10.1016/j.apsusc.2018.09.230 . hal-01972335

HAL Id: hal-01972335

<https://hal.science/hal-01972335v1>

Submitted on 30 Apr 2020

HAL is a multi-disciplinary open access archive for the deposit and dissemination of scientific research documents, whether they are published or not. The documents may come from teaching and research institutions in France or abroad, or from public or private research centers.

L'archive ouverte pluridisciplinaire **HAL**, est destinée au dépôt et à la diffusion de documents scientifiques de niveau recherche, publiés ou non, émanant des établissements d'enseignement et de recherche français ou étrangers, des laboratoires publics ou privés.



Distributed under a Creative Commons Attribution 4.0 International License

Nanostructure and photocatalytic properties of TiO₂ films deposited at low temperature by pulsed PECVD

D. Li ^{a,c}, S. Bulou ^b, N. Gautier ^a, S. Elisabeth ^a, A. Goulet ^b, M. Richard-Plouet ^a, P. Choquet ^b, A. Granier ^a

^a *Institut des Matériaux Jean Rouxel (IMN), Université de Nantes, CNRS, 2 rue de la Houssinière, BP 32229
44322 Nantes, France*

^b *Luxembourg Institute of Science and Technology, 5 avenue des Hauts-Fourneaux, L-4362 Esch-sur-Alzette,
Luxembourg,*

^c *College of Mechanical Engineering, Yangzhou University, Yangzhou 225127, China*

Abstract

The nanostructure and photocatalytic properties of TiO₂ thin films deposited by PECVD on silicon substrates were investigated. The films were grown at low temperature (< 120 °C) in an rf inductively coupled oxygen/titanium tetraisopropoxide plasma, in continuous and pulsed modes with different plasma-on time (via variation of the duty cycle, DC). All the films exhibit nano-columnar structures, but the reduction of plasma-on time by decreasing the duty cycle for pulsed mode leads to a more homogenous morphology with a diminished column size, and a decrease in the surface roughness. TiO₂ layers containing a high amount of anatase were grown at substrate temperatures less than 100 °C corresponding to $DC \geq 40\%$, then the crystallization was hindered with the decrease of DC, even inducing amorphous films for $DC \leq 10\%$. Moreover, the films deposited below 100 °C with deposition conditions where $50\% \leq DC \leq 75\%$ were shown to present a high photocatalytic activity, likely due to the presence of anatase crystalline nanocolumns at the surface.

Keywords: PECVD; pulsed plasma; TiO₂; anatase; TEM; photocatalytic activity.

1. Introduction

TiO₂ thin films have attracted intensive research as photocatalysts for their advantages in chemical stability, non-toxicity, commercial availability at a low cost and high photocatalytic activity [1-3]. The TiO₂ properties are due to its crystalline form which is mainly encountered as three phases including tetragonal anatase, tetragonal rutile and orthorhombic brookite [4]. TiO₂ exhibits different band gap energies for its different phases, viz. anatase (3.2 eV), rutile (3 eV) and brookite (3.1 eV) [5-8]. In addition to the effect of TiO₂ crystallization, some other essential factors such as grain size, preferred grain orientation, presence of structure defects and capability to absorb hydroxyl groups in the initial phase of excitation may also affect the photocatalytic activity [9-11]. Powders suspended in polluted solution due to their higher specific area may lead to more efficient photocatalytic properties, however films do not require filtering to be recovered after the volume to be depolluted has been treated. These films can be prepared by using different methods including sol-gel method [12-19], which is the most often used to synthesize TiO₂ thin films for photocatalytic applications. However other strategies were also largely investigated, such as liquid phase deposition [20], magnetron sputtering [21-23], atomic layer deposition [24], spray pyrolysis [25], chemical vapor deposition [26], metalorganic chemical vapor deposition [27] and plasma enhanced chemical vapor deposition (PECVD) [28-32]. Each method may lead to the growth of particular structure and film morphology, which may be quite distinctive and very difficult to repeat with another method. These particularities, on the other hand, may have a substantial effect on the overall photocatalytic activity of the material.

In the literature, titanium dioxide in anatase is generally reported to be obtained at high temperature, in the range of 400-600 °C [33]. However, plasma assisted deposition

(magnetron sputtering, PECVD) is known to allow decreasing the deposition temperature of many materials due to the bombardment of the growing film by energetic neutral and charged species. Nevertheless, in the case of TiO_2 , the deposition of anatase thin films by magnetron sputtering or PECVD below $150\text{ }^\circ\text{C}$ was reported by only few authors [23, 34].

In our previous studies, PECVD processes were used to yield some nanocolumnar structures with different phases including amorphous, anatase and rutile [35-36]. Actually these processes exhibit favorable features such as low deposition temperature, good film adhesion, high purity, good step coverage and easy control of reaction parameters [28, 37]. Enhancement of chemical reactions by means of low temperature plasma has been known and used for many years. In particular, some new nanostructured materials that cannot be obtained under equilibrium conditions could be prepared using chemical reaction under non equilibrium conditions [38-41], and in the area of property-altering surface coatings [42-43]. For photocatalytic applications, in order to reduce the substrate temperature during deposition while maintaining a sufficient energy input to obtain TiO_2 in crystallized form, the PECVD deposition can be controlled in pulsed plasma mode. In this mode, the electrical power is periodically applied to the gas, so that two times are then defined: the discharge time, when the power is applied for a time denoted T_{on} , and the post-discharge time, when the power is switched off for a time denoted T_{off} . Varying the plasma-on time to the period time has two important effects [44-45]: (1) to vary the mean power coupled to the plasma and hence the deposition temperature; (2) to allow the control of the ion to neutral flux ratio, which strongly influences the nanostructure and crystallinity.

In this work, we investigate the influence of the duty cycle (DC), defined as the discharge time to the period ratio, on the structural and photocatalytic properties of the TiO_2 films

deposited on silicon substrates in pulsed PECVD mode. The latter are also compared to the film deposited in continuous mode. The aim is both to gain insight into the influence of pulsed parameters on the structure of the deposited films by transmission electron microscopy (TEM), scanning electron microscopy (SEM), atomic force microscopy (AFM), X-ray diffraction (XRD), Raman spectroscopy and to deposit TiO₂ films with high photocatalytic activity at low temperature (typically below 100 °C).

2. Experimental

In this study, TiO₂ films were deposited on silicon (100) substrate (Si, supplied by Codex International, purity > 99.9999999%, CAS Number: 7440-21-3) using a low pressure high density radiofrequency (13.56 MHz) plasma process which is made of a plasma source connected to the diffusion chamber where a substrate is positioned. The rf inductively coupled plasma (ICP) source was generated by applying an rf power (400 W) to an external helicon antenna. Oxygen was introduced at the top of the plasma source. Titanium tetraisopropoxide [Ti(OC₃H₇)₄, TTIP, purity 99.999%, CAS Number: 546-68-9, supplied by Sigma Aldrich Ltd.], used as the titanium precursor, was injected into the diffusion chamber through a dispersal ring above the substrate holder. The flow rates of pure TTIP and oxygen were fixed at 0.24 sccm and 16 sccm, respectively, which corresponds to a 98.5:1.5 O₂/TTIP mixture, while the total working pressure was fixed at 0.4 Pa. The O₂/TTIP plasmas can be operated either in continuous (CW) or pulsed mode. In this study the frequency was fixed at 1 kHz and the duty cycle (DC) was varied from 10 to 75% by tuning the T_{on} time. The thickness lies between 250 and 300 nm for all deposited films. The substrate temperature was measured using temperature sensitive labels stuck on the back side of the Si substrates [46]. It was measured to be around 120 °C in continuous (CW) standard plasma conditions and was

shown to be decreased in the pulsed mode down to 80 °C for DC=50% and below 50 °C for DC = 25%. The deposition parameters are summarized in Table 1.

Table 1. Growth conditions of TiO₂ films using the pulsed PECVD system.

rf power coupled to the ICP source	400 W
Working pressure	0.4 Pa
Flow rate of TTIP	0.24 sccm
Flow rate of O ₂	16 sccm
Pulsed mode frequency	1 kHz
Duty cycle (DC) for pulsed mode	10%, 25%, 40%, 50%, 75%, CW
Substrate temperature (± 5 °C)	< 50, < 50, 50, 80, 90, 120
Substrate	Si (100)

The film morphology was observed by SEM using a JEOL-type JSM 7600F, operating at 10 kV. TEM analysis was performed using a Hitachi H9000-NAR microscope (LaB₆ filament, 300 kV, point to point resolution: 0.18 nm). Cross-section TEM samples were prepared by tripod polishing and afterwards by Ar⁺ ion polishing using Gatan precision ion polishing system (PIPS). The crystalline nature of all the films was determined by X-Ray diffraction (XRD) and Raman spectroscopy. XRD measurements were carried out on a Siemens D8 using Cu K α radiation (K α = 1.5406 Å) operating in $\theta/2\theta$ configuration, in the 2θ range of 20-60 °, with a step of 0.03 ° and a dwell of 15 s/step. TiO₂ anatase peaks were attributed thanks to JCPDS file number 89-4921. The Raman spectra were recorded with a Renishaw inVia micro-Raman spectrometer at an excitation wavelength of 532 nm with a laser power of approximately 0.44 mW focused on a 1 μm^2 spot. The film surface topography was observed by atomic force microscopy (AFM, NanoWizard II, JPK Instruments) in the contact mode.

The photocatalytic activity of the as-deposited TiO₂ films was studied by measuring stearic acid (SA) decomposition under UV exposure (Herolab UV-8 SL, 254 nm, 8 W). In order to deposit stearic acid on the entire surface of the sample, it was diluted in methanol (0.02 mol L⁻¹) and deposited by spin coating. 10 microliters were deposited on the coatings (1 cm²) and

spin-coated for 30 seconds at 10000 rpm. The samples were then stored in dark in a black box for at least 3 hours before being exposed to the light source. The samples were then illuminated by an UV lamp. The UV lamp (Herolab UV-8 SL, 254 nm, 8 W) was positioned 20 cm above the samples, corresponding to a calculated irradiance of ca. 0.38 mW cm^{-2} (i.e. $4.9 \times 10^{14} \text{ photons.s}^{-1} \text{ cm}^{-2}$) illuminating the samples surface [47].

The decomposition of the stearic acid was assessed using FTIR spectroscopy (Bruker VERTEX 70 in transmission) by measuring the integrated area of absorption bands in the range $2800\text{-}3000 \text{ cm}^{-1}$ (C-H stretching modes of the stearic acid). The photodegradation efficiency was evaluated through the monitoring of this absorption band area as a function of illumination duration. The linear regression of the corresponding degradation curves gives a photocatalytic efficiency ($\text{cm}^{-1} \text{ h}^{-1}$).

Besides, the FTIR absorption in the range $2800\text{-}3000 \text{ cm}^{-1}$ is linked to the quantity of SA by a conversion factor δ , which gives an equivalency between a number of molecules of SA per cm^2 and an integrated FTIR area value of 1 cm^{-1} . A conversion factor value of $\delta = 9.7 \times 10^{15} \text{ molecules of SA cm}^{-2} \text{ per cm}^{-1}$ of FTIR absorption is used in this article [48]. This allows us to calculate an UV light activity R_{SA} defined as the number of molecules cm^{-2} of SA degraded per second.

3. Results

3.1 Film morphology

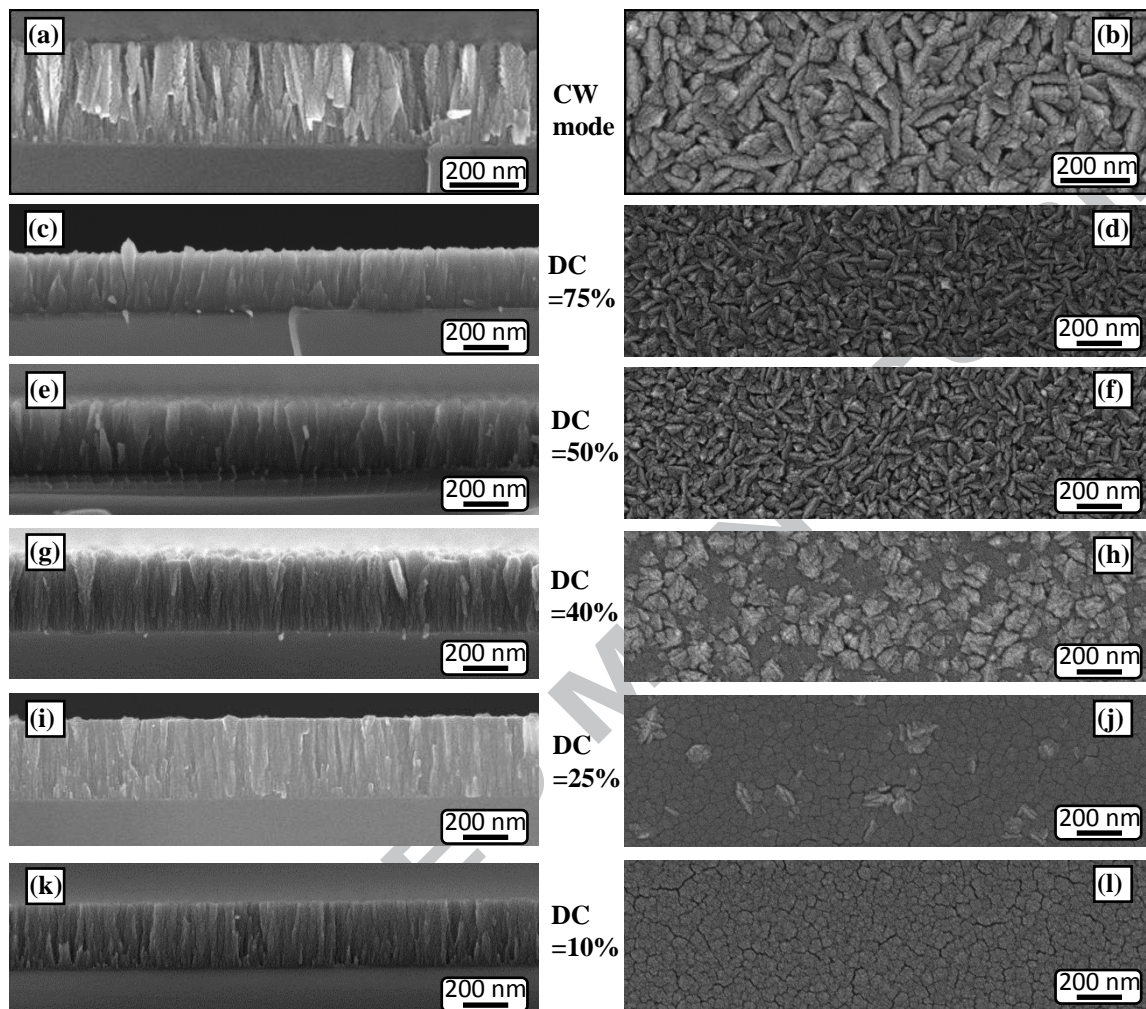
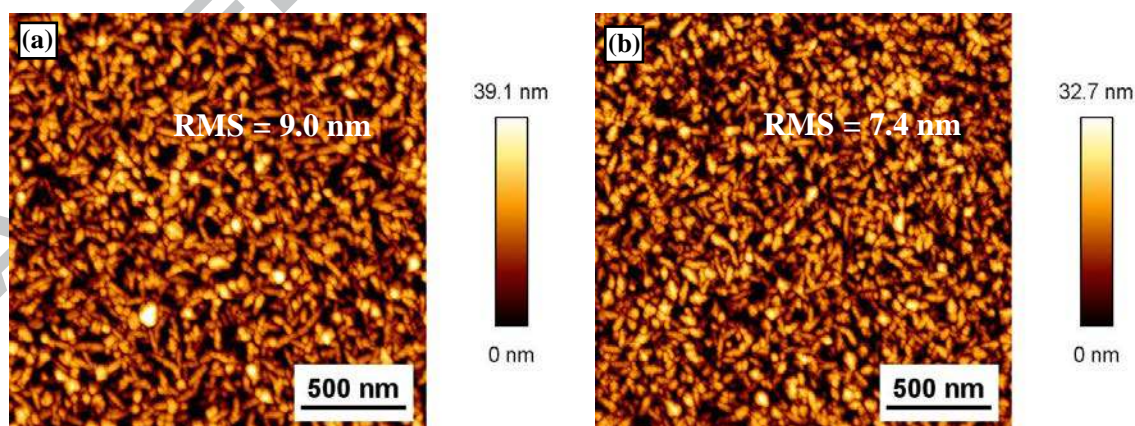


Fig. 1. SEM micrographs of the TiO_2 films deposited with different duty cycles for pulsed and continuous mode (100%). (a, b) continuous mode, (c, d) DC = 75%, (e, f) DC = 50%, (g, h) DC = 40%, (i, j) DC = 25%, (k, l) DC = 10%, (a, c, e, g, i, k) SEM side-views, (b, d, f, h, j, l) SEM top-views.

SEM micrographs including side-views and top-views of the TiO_2 films deposited in continuous mode and in pulsed mode for different duty cycles are displayed in Fig. 1. All the films exhibit columnar structures, but it seems that the column size can be decreased as the duty cycle is reduced which can be identified by TEM in details. The CW mode leads to a typical morphology on Si substrate in agreement with previous studies [35], which is the gradient columnar structure including a dense sublayer at the interface and a disordered

columnar top layer. The morphologies for the films grown in the pulsed mode with $DC \geq 40\%$ retain the same gradient columnar structure, but the degree of homogeneity in the growth direction is improved as DC is decreased. Moreover, when $DC < 40\%$, the columns appear more organized and the whole morphology seems to be homogenous along the growth direction.

The evolution of cross-sectional morphology is also reflected in the surface topography (see Fig. 2), for the films deposited at $DC > 40\%$, the top surfaces are quite rough because of the disordered columns leading to some clustering of grains till the surface. Moreover, the RMS roughness value decreases with DC, from 9.0 nm for CW mode to 6.0 nm for $DC = 50\%$. But in the case of $DC = 40\%$, the surface topography marks a transition with the gradually disappearance of the clusters leading to an abrupt increase in roughness up to 11.2 nm. The images of the surfaces of the TiO_2 films reveal a change from granular clusters to rice-shaped grains as DC is further decreased below 40%, and the grain size is also reduced with DC leading to smoother top surfaces, the roughness is even decreased down to 4.0 nm for $DC = 25\%$.



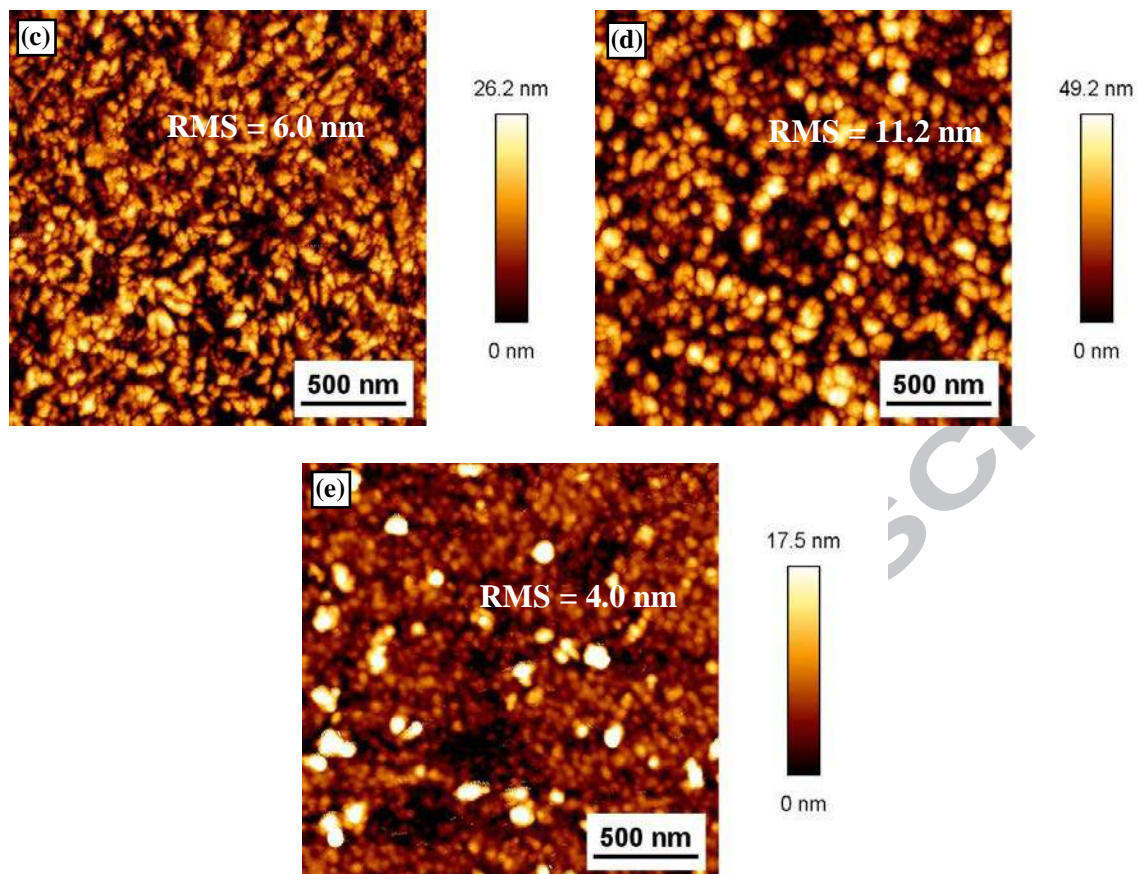


Fig. 2. AFM measurements of the TiO₂ films deposited with different duty cycles for pulsed and continuous mode (100%). (a) continuous mode, (b) DC = 75%, (c) DC = 50%, (d) DC = 40%, (e) DC = 25%.

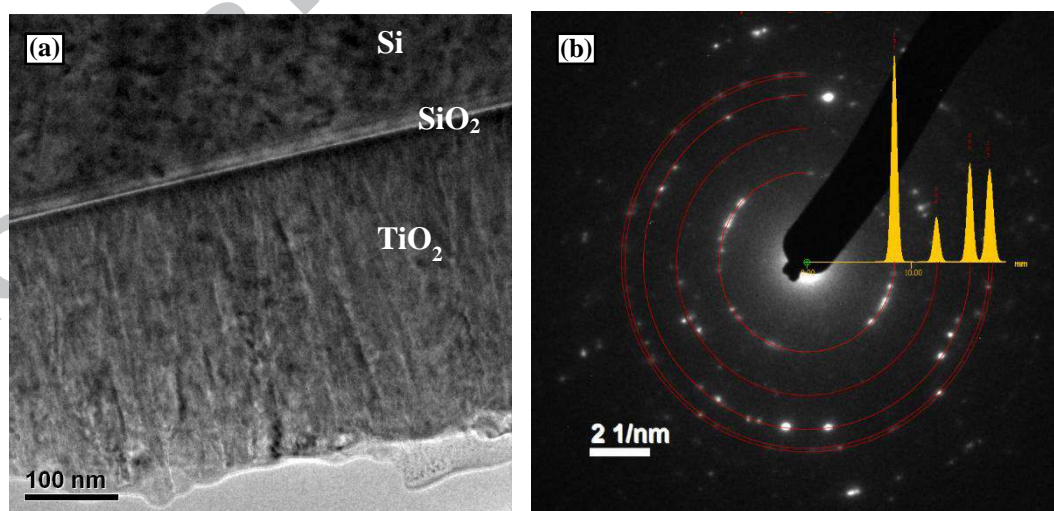


Fig. 3. TEM on the TiO₂ film deposited in the continuous mode (CW). (a) The whole film morphology, (b) selected area electronic diffractions (SAED): experimental diffraction of the film and simulation for anatase using JEMS software [49].

The TEM image (in Fig. 3) of a 300 nm-thick TiO₂ film deposited in the CW mode on Si substrate clearly shows a highly crystallized film with a columnar morphology. The interface between the Si (100) substrate with a ~4 nm native amorphous SiO₂ layer and the polycrystalline TiO₂ film was identified in Fig. 3(a). The SAED pattern (Fig. 3(b)) is typical for the anatase phase. The presence of a dense layer topped with a columnar crystallized film is quite consistent with SEM pictures which indicated the presence of a dense film topped with a gradient layer [35].

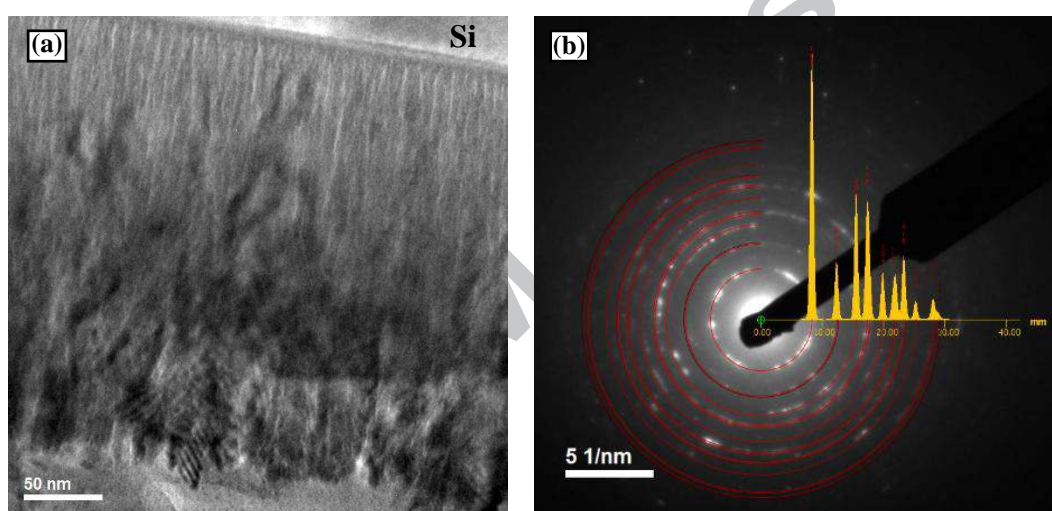


Fig. 4. TEM on the TiO₂ film deposited with the duty cycle of 50% for pulsed mode. (a) The whole film morphology, (b) selected area electronic diffractions (SAED): experimental diffraction of the film and simulation for anatase using JEMS software.

The TEM study of the TiO₂ film deposited in the pulsed mode (DC = 50%) displayed in Fig. 4 shows that using pulsed plasma allows decreasing the deposition temperature (measured to be less than 80 °C) while conserving anatase crystallites (in Fig. 4(b)). Compared to the CW mode, a similar columnar morphology was observed, but a slight decrease in the column diameter from ~30 to ~15 nm was observed for the pulsed mode.

Pulsing the plasma decreases the mean energy transferred to the substrate over a whole period ($T_{\text{on}} + T_{\text{off}}$) (due to a decrease in the heat and ion fluxes during T_{off}), which affects the surface

of the growing film and causes a reorganization of the surface atoms. Thus, the reduction of plasma deposition time by decreasing the duty cycle for pulsed mode leads to a more homogenous columnar morphology with a decreased column size and a decrease in the surface roughness.

3.2 Film crystallization

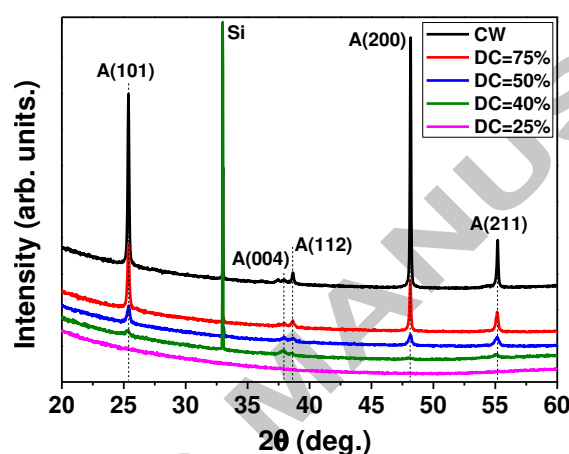


Fig. 5. XRD patterns of the TiO_2 films deposited with different duty cycles for pulsed mode and continuous mode.

As can be seen in the XRD patterns displayed in Fig. 5, the as-deposited film in the continuous mode crystallizes in the anatase variety as demonstrated through the appearing of diffraction peaks at 25.5° , 37.8° , 38.6° , 48.1° and 55.1° , corresponding to lattice planes (101), (004), (112), (200) and (211), respectively. There is a preferential orientation along the (200) direction in the CW mode, while polycrystalline anatase is produced in pulsed mode. The intensities of the anatase peaks were weakened as DC decreased, and disappeared at DC = 25%, where no peak was detected meaning that the film is amorphous. The crystallization of the films was further investigated by Raman spectroscopy which is very sensitive to low amount of anatase and in our conditions provides more local information than XRD.

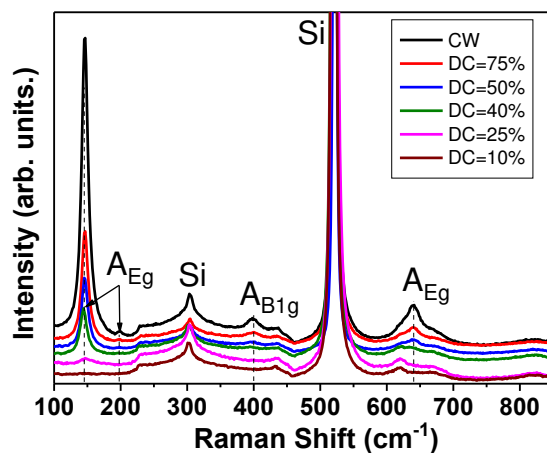


Fig. 6. Raman spectra of the TiO₂ films prepared with different duty cycles for pulsed mode and continuous mode (CW).

Fig. 6 shows the evolution of the Raman spectra of the TiO₂ films deposited with different duty cycles for pulsed mode and continuous mode. For the TiO₂ films grown in the CW mode and the pulsed mode with $DC \geq 40\%$, the spectra exhibit five peaks at 144, 198, 395, 516 and 640 cm^{-1} which are characteristic of the anatase phase and assigned to E_g , B_{1g} , A_{1g} and E_g modes [50]. However, in the case of $DC = 25\%$, the characteristic peaks of anatase are very weak in intensity, but the peak at 144 cm^{-1} is clearly observed which suggests that the film may consist in a small amount of anatase dispersed in an amorphous matrix. For the films deposited at $DC = 10\%$, the Raman spectra did not show any indication of crystallized TiO₂.

In the case of CW mode, ions in the plasma can be continuously generated to participate in the crystallization of the growing film with a simultaneous release of energy which is helpful for the anatase formation. However, in the pulsed mode, the flux and energy of the ion bombardment are no longer generated in post-discharge, which may lead to a reduction in the crystallization rate by increasing the plasma-off time. In addition, the probable phenomenon of hydrolysis of TTIP during post-discharge can also hamper the crystallization, as this reaction is thus carried out in thermodynamic equilibrium and tends to create amorphous TiO₂ [51].

Therefore, a reduction of the amount of the crystallized anatase phase is observed when the duty cycle is decreased. This statement can indicate that the growth of anatase crystalline nanocolumns is directly linked to the deposition period during the plasma on time, independently of the substrate temperature.

3.3 Photocatalytic activity

According to the above discussion concerning the influence of pulsed plasmas on the TiO₂ film morphology and crystallization, some interesting points about the anatase content, columns size and organization, surface state were demonstrated, which may affect the photocatalytic properties of these TiO₂ films. In this work, the photocatalytic activity of thin films was evaluated by monitoring of the degradation of stearic acid under UV light.

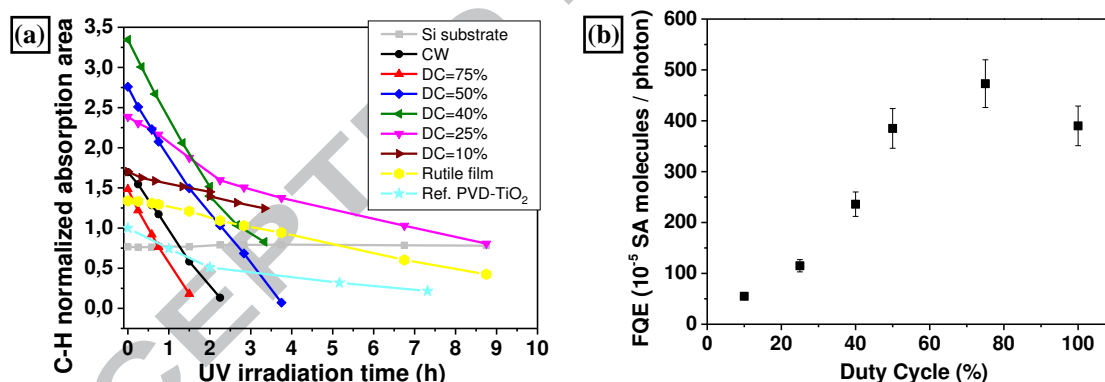


Fig. 7. Evolution of photocatalytic activity for the TiO₂ films grown with different duty cycles for pulsed mode and continuous mode (100%), and compared with the reference TiO₂ film deposited by PVD and PECVD-rutile films. (a) C-H absorption integrated area (2800-3000 cm⁻¹) versus UV illumination time, (continuous lines are just guidelines to get a better view of the evolutions) (b) Formal Quantum Efficiency for SA molecules calculated from SA degradation rate as a function of the duty cycles.

Fig. 7 presents the evolution of the integrated area of the FTIR absorption band in the range 2800-3000 cm⁻¹ as a function of the exposure duration to UV illumination on the TiO₂ films deposited in continuous and pulsed modes. These measurements were also compared to

photocatalytic performance (with the same measuring device) of bare silicon substrate, PECVD-grown rutile films [35] and 2 μm TiO_2 film obtained by magnetron sputtering (PVD) at 250 $^\circ\text{C}$ [52]. One can note that the silicon substrate has no photocatalytic activity (as expected), whereas the films presented in this work all exhibit a decrease of the SA quantity when illuminated by UV light.

In order to compare with available literature data, the formal quantum efficiency (FQE) for SA is calculated [48] and presented in Fig. 7(b). The FQE is calculated as the number of SA photodegraded by the incident photons (see eq. 1). The slope of the degradation curve of SA, R_{SA} and FQE for the films deposited under different conditions are shown in Table 2.

(eq. 1)

Table 2. Evolution of the SA degradation rate, R_{SA} and FQE for the TiO_2 films grown with different duty cycles for pulsed mode and continuous mode (100%).

Duty cycle	SA degradation rate (h^{-1})	R_{SA} (SA, 254 nm) (molecules $\text{cm}^{-2}\text{s}^{-1}$)	FQE (SA, 254 nm) (10^{-5} molecules/photon)
100 % (CW)	0.71 ± 0.7	$(1.9 \pm 0.2) \times 10^{12}$	390 ± 39
75 %	0.86 ± 0.9	$(2.3 \pm 0.3) \times 10^{12}$	473 ± 47
50 %	0.7 ± 0.7	$(1.9 \pm 0.2) \times 10^{12}$	385 ± 39
40 %	0.43 ± 0.4	$(1.2 \pm 0.1) \times 10^{12}$	236 ± 24
25 %	0.21 ± 0.2	$(5.7 \pm 0.6) \times 10^{11}$	115 ± 12
10 %	0.1 ± 0.01	$(2.7 \pm 0.3) \times 10^{11}$	55 ± 6

The reproducibility of photocatalytic activity measurements was confirmed for several samples deposited for DC = 100, 75 and 50%.

The photodegradation efficiency of TiO_2 films containing anatase deposited at DC = 100%, 75% and 50% exhibits very high values, with FQE equal to 390×10^{-5} , 473×10^{-5} and 385×10^{-5}

molecules/photon respectively. These values are very good as they surpass the FQE of some reference films such as P25 TiO₂ and Pilkington Activ thin films, which exhibit FQE values of 256×10^{-5} and 10×10^{-5} respectively [53].

Nevertheless, photocatalysis is somehow dependent on the coating thickness. Indeed, thicker films induced a higher probability of producing reactive species that participate to catalytic processes. In this article, thin films have a thickness of ca. 250 nm, whereas in the article of A. Mills et al [53], P25 TiO₂ and Pilkington Activ have a thickness of 90 nm and 15 nm respectively. One can note the slightly higher photocatalytic activity of the samples obtained at DC = 50%, 75 % and 100% which might be due to more anatase content and higher surface area, induced by smaller column size and higher roughness. It is then noted that the photocatalytic activity decreases when DC decreases reaching FQE = 236×10^{15} , 115×10^{15} and 55×10^{15} molecules per photon for DC = 40 %, 25 % and 10 % respectively. Although these films have lower photoactivity, their efficiency is still good especially when considering the very low substrate temperature (< 50 °C) during deposition.

TiO₂ layers deposited for DC \geq 50% contain a significant amount of anatase and present the highest photocatalytic activity. Although the TiO₂ layer grown at DC = 40% has a quite rough top surface, the crystalline anatase content detected by Raman scattering and XRD is high enough to lead to a lower but still significant photocatalytic activity. In the cases of DC = 25 and 10%, TiO₂ layers have a reduced but still significant conversion rate which is higher than the PVD-deposited anatase at 250 °C [52]. Indeed, the R_{SA} of the film obtained at DC = 10%, at a temperature < 50 °C is comparable to other films obtained using an atmospheric pressure PECVD process with substrate temperature around 100 °C [54]. Moreover, the rutile TiO₂ film deposited by PECVD shows a rather poor photodegradation efficiency.

This study has demonstrated that it is possible to deposit TiO₂ layers with high photocatalytic activity at temperatures below 100 °C ($50\% \leq DC \leq 75\%$). This therefore opens up interesting

prospects for the deposition of photocatalytic layers, for example on flexible polymer substrates.

4. Conclusions

Highly efficient photocatalytic anatase nanocolumnar TiO₂ thin films were successfully deposited by pulsed-PECVD process at relatively low temperature less than 100 °C on Si substrate. The effect of plasma-off time by tuning the duty cycle of pulsed mode was investigated on TiO₂ thin films in view of improving their photocatalytic properties. The efficient photocatalytic property of such a film depends on the presence of the anatase phase at its surface and also its roughness and microstructure. At a duty cycle between 40% and 100%, the bombardment of the particles at the substrate is strong enough for inducing mobility of surface particles, promoting the formation of crystalline anatase TiO₂ films with disordered columnar morphologies. The photocatalytic activity for these films is very high. As DC is decreased below 40%, the accumulation of impact energy and heat is insufficient, leading to the formation of a surface including only a small amount of anatase embedded in an amorphous film, which has relatively smooth surface and homogeneous columns along the growth direction. Thus the photocatalytic activity is reduced, but is still significant regarding the low substrate temperature.

Acknowledgments

Acknowledgements for the master students: Theo Leclerq (mainly) for this paper. The work of Dayu Li is supported by the National Natural Science Foundation of China (51602279), High-end Talents and Young Backbone Teacher Project of Yangzhou University.

References

- [1]. M. Nasr, C. Eid, R. Habchi, P. Miele, M. Bechelany, Recent progress on titanium dioxide nanomaterials for photocatalytic applications, *ChemSusChem* 11 (2018) 1-26.
- [2]. L. Chen, M.E. Graham, G. Li, K.A. Gray, Fabricating highly active mixed phase TiO₂ photocatalysts by reactive DC magnetron sputter deposition, *Thin Solid Films* 515 (2006) 1176-1181.
- [3]. C.H. Lu, W.H. Wu, R.B. Kale, Synthesis of photocatalytic TiO₂ thin films via the high-pressure crystallization process at low temperatures, *J. Hazard. Mater.* 147 (2007) 213-218.
- [4]. H.C. Lee, W.S. Hwang, Substrate effects on the oxygen gas sensing properties of SnO₂/TiO₂ thin films, *Appl. Surf. Sci.* 253 (2006) 1889-1897.
- [5]. L. Sang, Y. Zhao, C. Burda, TiO₂ nanoparticles as functional building blocks, *Chem. Rev.* 114 (2014) 9283-9318.
- [6]. J. Xu, L. Li, Y. Yan, H. Wang, X. Wang, X. Fu, G. Li, Synthesis and photoluminescence of well-dispersible anatase TiO₂ nanoparticles, *J. Colloid Interf. Sci.* 318 (2008) 29-34.
- [7]. K. Nagaveni, G. Sivalingam, M.S. Hegde, G. Madras, Solar photocatalytic degradation of dyes: high activity of combustion synthesized nano TiO₂, *Appl. Catal., B Environ.* 48 (2004) 83-93.
- [8]. S. Yin, Q. Zhang, F. Saito, T. Sato, Preparation of visible light-activated titania photocatalyst by mechanochemical method, *Chem. Lett.* 32 (2003) 358-359.
- [9]. D.C. Hurum, A.G. Agrios, K.A. Gray, T. Rajh, C. Thurnauer, Explaining the enhanced photocatalytic activity of degussa P25 mixed-phase TiO₂ using EPR, *J. Phys. Chem. B* 107 (2003) 4545-4549.
- [10]. T. Luttrell, S. Halpegamage, J. Tao, A. Kramer, E. Sutter, M. Batzill, Why is anatase a better photocatalyst than rutile? – Model studies on epitaxial TiO₂ films, *Sci. Rep.* 4 (2014) 4043.
- [11]. H. Ogawa, T. Higuchi, A. Nakamura, S. Tokita, D. Miyazaki, T. Hattori, T. Tsukamoto, Growth of TiO₂ thin film by reactive RF magnetron sputtering using oxygen radical, *J. Alloy. Compd.* 449 (2008) 375-378.
- [12]. M. Grätzel, Sol-gel processed TiO₂ films for photovoltaic applications, *J. Sol-Gel Sci. Technol.* 22 (2001) 7-13.
- [13]. C.C. Trepalis, P. Keivanidis, G. Kordas, M. Zaharescu, M. Crisan, A. Szatvanyi, M. Gartner, TiO₂(Fe³⁺) nanostructured thin films with antibacterial properties, *Thin Solid Films* 433 (2003) 186.
- [14]. A. Rachel, M. Subrahmanyam, P. Boule, Comparison of photocatalytic efficiencies of TiO₂ in suspended and immobilised form for the photocatalytic degradation of nitrobenzenesulfonic acids, *Appl. Catal., B Environ.* 37 (2002) 301.

- [15]. S. Senthilkumar, K. Porkodi, R. Vidyalakshmi, Photodegradation of a textile dye catalyzed by sol-gel derived nanocrystalline TiO₂ via ultrasonic irradiation, *J. Photochem. Photobiol., A Chem.* 170 (2005) 225.
- [16]. P.A. Christensen, T.P. Curtis, T.A. Egerton, S.A.M. Kosa, J.R. Tinlin, Photoelectrocatalytic and photocatalytic disinfection of *E. coli* suspensions by titanium dioxide, *Appl. Catal., B Environ.* 41 (2003) 371.
- [17]. K. Sunada, T. Watanabe, K. Hashimoto, Studies on photokilling of bacteria on TiO₂ thin film, *J. Photochem. Photobiol., A Chem.* 156 (2003) 227.
- [18]. A. Mills, A. Lepre, N. Elliott, S. Bhopal, I.P. Parkin, S.A. O'Neill, Characterisation of the photocatalyst Pilkington Activ™: a reference film photocatalyst? *J. Photochem. Photobiol., A Chem.* 160 (2003) 213.
- [19]. A. Mills, G. Hill, S. Bhopal, I.P. Parkin, S.A. O'Neill, Thick titanium dioxide films for semiconductor photocatalysis, *J. Photochem. Photobiol., A Chem.* 160 (2003) 185.
- [20]. J.G. Yu, H.G. Yu, B. Cheng, X.J. Zhao, J.C. Yu, W.K. Ho, The effect of calcination temperature on the surface microstructure and photocatalytic activity of TiO₂ thin films prepared by liquid phase deposition, *J. Phys. Chem. B* 107 (2003) 13871-13879.
- [21]. D. Mardare, M. Tasca, M. Delibas, G.I. Rusu, On the structural properties and optical transmittance of TiO₂ r.f. sputtered thin films, *Appl. Surf. Sci.* 156(2000) 200-206.
- [22]. W. Zhang, S. Zhu, Y. Li, F. Wang, Photocatalytic property of TiO₂ films deposited by pulsed DC magnetron sputtering, *J. Mater. Sci. Technol.* 20(2004) 31-34.
- [23]. S. Daviosdottir, R. Shabadi, A.C. Galca, I.H. Andersend, K. Dirscherl, R. Ambata, Investigation of DC magnetron-sputtered TiO₂ coatings: effect of coating thickness, structure, and morphology on photocatalytic activity, *Appl. Surf. Sci.* 313 (2014) 677-686.
- [24]. V. Pore, A. Rahtu, M. Leskela, M. Ritala, T. Sajavaara, J. Keinonen, Atomic layer deposition of photocatalytic TiO₂ thin films from titanium tetramethoxide and water, *Chem. Vap. Depos.* 10 (2004) 143-148.
- [25]. M. Miki-Yoshida, V. Collins-Martinez, P. Amèzaga-Madrid, A. Aguilar-Elguèzabal, Thin films of photocatalytic TiO₂ and ZnO deposited inside a tubing by spray pyrolysis, *Thin Solid Films* 419 (2002) 60.
- [26]. A. Mills, N. Elliott, I.P. Parkin, S.A.O. Neill, R.J. Clark, Novel TiO₂ CVD films for semiconductor photocatalysis, *J. Photochem. Photobiol., A Chem.* 151 (2002) 171.

- [27]. O.J. Jung, S.H. Kim, K.H. Cheong, W. Li, S.J. Saha, Metallorganic Chemical Vapor Deposition and Characterization of TiO₂ Nanoparticles, *Bull. Korean Chem. Soc.* 24 (2003) 49.
- [28]. G.A. Battiston, R. Gerbasi, A. Gregori, M. Porchia, S. Cattarin, G.A. Rizzi, PECVD of amorphous TiO₂ thin films: effect of growth temperature and plasma gas composition, *Thin Solid Films* 371 (2000) 126-131.
- [29]. K. Baba, S. Bulou, M. Quesada-Gonzalez, S. Bonot, D. Collard, N.D. Boscher, P. Choquet, Significance of a noble metal nanolayer on the UV and visible light photocatalytic activity of anatase TiO₂ thin films grown from a scalable PECVD/PVD approach, *ACS Appl. Mater. Interfaces* 9 (2017) 41200–41209.
- [30]. K. Baba, S. Bulou, P. Choquet, N.D. Boscher, Photocatalytic anatase TiO₂ thin films on polymer optical fiber using atmospheric-pressure plasma, *ACS Appl. Mater. Interfaces* 9 (2017) 13733–13741.
- [31]. M. Maeda, T. Watanabe, Evaluation of photocatalytic properties of titanium oxide films prepared by plasma-enhanced chemical vapor deposition, *Thin Solid Films* 489 (2005) 320-324.
- [32]. V. Rico, P. Romero, J.L. Hueso, J.P. Espinós, A.R. González-Elipé, Wetting angles and photocatalytic activities of illuminated TiO₂ thin films, *Catal. Today* 143 (2009) 3470-354.
- [33]. A. Dorian, H. Hanaor, C.C. Sorrell, Review of the anatase to rutile phase transformation, *J. Mater. Sci.* 46 (2011) 855-874.
- [34]. A. Kolouch, P. Hájková, A. Macková, M. Horáková, J. Houdková, P. Špatenka, S. Hucek, Photocatalytic TiO₂ thin Film Prepared by PE CVD at low Temperature, *Plasma Process. Polym.* 4 (2007) S350-S355.
- [35]. D. Li, M. Carette, A. Granier, J. P. Landesman, A. Gouillet, Effect of ion bombardment on the structural and optical properties of TiO₂ thin films deposited from oxygen/titanium tetraisopropoxide inductively coupled plasma, *Thin Solid Films* 589 (2015) 783.
- [36]. D. Li, S. Elisabeth, A. Granier, M. Carette, A. Gouillet, J. P. Landesman, Structural and optical properties of PECVD TiO₂-SiO₂ mixed oxide films for optical applications, *Plasma Process. Polym.* 13 (2016) 918-928.
- [37]. W.G. Lee, S.I. Woo, J.C. Kim, S.H. Choi, K.H. Oh, Preparation and properties of amorphous TiO₂ thin films by plasma enhanced chemical vapor deposition, *Thin Solid Films* 237 (1994) 105.
- [38]. L. Martinu, D. Poitras, Plasma deposition of optical films and coatings: A review, *J. Vac. Sci. Technol., A* 18 (2000) 2619.

- [39]. M.L. Hitchman, K.F. Jensen, Chemical vapor deposition: principles and applications, Academic Press, London, 1993.
- [40]. H. Szymanowski, O. Zabeida, J.E. Klemberg-Sapieha, L. Martinu, Optical properties and microstructure of plasma deposited Ta₂O₅ and Nb₂O₅ films, *J. Vac. Sci. Technol.*, A 23 (2005) 241.
- [41]. S. Larouche, H. Szymanowski, J.E. Klemberg-Sapieha, L. Martinu, S.C. Gujrathi, Microstructure of plasma-deposited SiO₂/TiO₂ optical films, *J. Vac. Sci. Technol. A* 22 (2004) 1200.
- [42]. A.M. Wróbel, Surface free energy of plasma-deposited thin polymer films, in: K.L. Mittal (Ed.), *Physicochemical Aspects of Polymer Surfaces*, vol. 1, Plenum Press, New York, 1981, p. 197.
- [43]. J. Behnisch, J. Tyczkowski, M. Gazicki, I. Pela, A. Holländer, R. Ledzion, Formation of hydrophobic layers on biologically degradable polymeric foils by plasma polymerization, *Surf. Coat. Technol.* 98 (1998) 872.
- [44]. Y. Wang, E.C. Benck, M. Misakian, M. Edamura, J.K. Olthoff, Time-resolved measurements of ion energy distributions and optical emissions in pulsed radio-frequency discharges, *J. Appl. Phys.* 87 (2000) 2114.
- [45]. M. Heintze, M. Magureanu, M. Kettlitz, Mechanism of C₂ hydrocarbon formation from methane in a pulsed microwave plasma, *J. Appl. Phys.* 92 (2002) 7022.
- [46]. S. Elisabeth, Ph.D. Thesis, University of Nantes, France, 2015.
- [47]. N.D. Boscher, S. Olivier, R. Maurau, S. Bulou, T. Sindzingre, T. Belmonte, P. Choquet, Photocatalytic anatase titanium dioxide thin films deposition by an atmospheric pressure blown arc discharge, *Appl. Surf. Sci.* 311 (2014) 721–728.
- [48]. A. Mills, J. Wang, Simultaneous monitoring of the destruction of stearic acid and generation of carbon dioxide by self-cleaning semiconductor photocatalytic films, *J. Photoch. Photobio. A* 182 (2006) 181–186.
- [49]. P. Stadelmann-JEMS Java Electron Microscopy Software-<http://cime.epfl.ch/> (2004).
- [50]. T. Ohsaka, F. Izumi, Y. Fujiki, Raman spectrum of anatase, TiO₂, *J. Raman Spectrosc.* 7 (1978) 321–324.
- [51]. D.A.H. Hanaor, I. Chironi, I. Karatchevtseva, G. Triani, C.C. Sorrell, Single and mixed phase TiO₂ powders prepared by excess hydrolysis of titanium alkoxide, *Adv. Appl. Ceram.* 111 (2012) 149–158.

- [52]. R. Maurau, N.D. Boscher, S. Olivier, S. Bulou, T. Belmonte, J. Dutroncy, T. Sindzingre, P. Choquet, Atmospheric pressure, low temperature deposition of photocatalytic TiO_x thin films with a blown arc discharge, *Surf. Coat. Technol.* 232 (2013) 159-165.
- [53]. A. Mills, A. Lepre, N. Elliott, S. Bhopal, I.P. Parkin, S.A. O'Neill, Characterisation of the photocatalyst Pilkington Activ™: a reference film photocatalyst? *J. Photoch. Photobio. A* 160 (2003) 213–224
- [54]. J.B. Chemin, S. Bulou, K. Baba, C. Fontaine, T. Sindzingre, N.D. Boscher, P. Choquet, Transparent anti-fogging and self-cleaning $\text{TiO}_2/\text{SiO}_2$ thin films on polymer substrates using atmospheric plasma, *Sci. Rep.* 8 (2018) 9603.